

Seismic risk assessment of staggered wall system structures

Jinkoo Kim* and Donggeol Baek

Department of Civil and Architectural Engineering, Sungkyunkwan University, 300 Cheoncheon-dong,
Jangan-gu, Suwon, 440-746, Korea

(Received May 15, 2013, Revised July 6, 2013, Accepted August 25, 2013)

Abstract. In this study the seismic risk assessments of six- and twelve-story staggered wall system structures with three different structural variations were performed. The performances of staggered wall structures with added columns along the central corridor and the structures with their first story walls replaced by beams and columns were compared with those of the regular staggered wall structures. To this end incremental dynamic analyses were carried out using twenty two pairs of earthquake records to obtain the failure probabilities for various intensity of seismic load. The seismic risk for each damage state was computed based on the fragility analysis results and the probability of occurrence of earthquake ground motions. According to the analysis results, it was observed that the structures with added columns along the central corridor showed lowest probability of failure and seismic risk. The structures with their first story walls replaced by beams and columns showed lowest margin for safety.

Keywords: staggered wall; seismic fragility; seismic hazard; seismic risk

1. Introduction

Staggered wall structures are structural systems for reinforced concrete residential buildings in which story-high walls extend across the entire width of the buildings. By staggering the locations of the walls on alternate floors, large clear areas are created on each floor. Floor slabs span only half the wall spacing, and the staggered walls can be pierced for openings or corridors. Similar system, the staggered truss system, has been applied in steel structures since 1970's. The staggered wall system was first proposed by Fintel (1968), who conducted experiments of half scale staggered wall structure subjected to gravity load. Mee *et al.* (1975) carried out shaking table tests of 1/15 scaled models for the staggered wall systems. Kim and Jun (2011) evaluated the seismic performance of partially staggered wall apartment buildings using non-linear static and dynamic analysis, and compared the results with those of conventional shear wall system apartment buildings. They found that the structure with partially staggered walls satisfied the collapse prevention performance objective required by the FEMA-356 and thus was considered to have enough capacity for design level seismic load. Recently Lee and Kim (2013) investigated the seismic performance of six and 12-storey staggered wall structures with a middle corridor based on the FEMA P695 procedure, and found that the analysis model structures have enough safety margin for collapse against design level earthquakes.

*Corresponding author, Professor, E-mail: jkim12@skku.edu

The seismic risk assessment and loss estimation is an essential step to seismic condition assessment and hazard reduction of various structures. Shinozuka *et al.* (2000) showed that analytical fragility curves are in reasonably good agreement with empirical curves obtained from observation of damaged structures. Ellingwood (2001) surveyed structural reliability methods for improving earthquake-resistant structural design and condition assessment practices. Cornell *et al.* (2002) presented a probabilistic framework for seismic design and assessment of structures and its application to steel moment-resisting frame buildings, which is the probabilistic basis for the 2000 SAC Federal Emergency Management Agency steel moment frame guidelines. Erberik and Elnashai (2004) derived fragility curves of medium-rise flat-slab buildings with masonry infill walls and compared the results with those derived for moment-resisting RC frames. Ellingwood and Wen (2005) proposed a risk-benefit-based analysis and seismic design procedure and applied it to buildings subjected to earthquake effects in Mid-America. Celik and Ellingwood (2009) presented a probability-based procedure for seismic vulnerability and risk assessment of RC frames designed only gravity load. Taflanidis and Jia (2011) developed a simulation-based framework for risk assessment and probabilistic sensitivity analysis of base isolated structures. Sorensen (2011) presented a theoretical framework for the design and analysis of robustness of timber structures. Ramirez *et al.* (2012) developed fragility functions for estimation of damage in pre-1994 welded flange bolted-web beam-to-column moment connections. Tafakori *et al.* (2013) proposed a risk-based optimal retrofit method of a tall steel building with friction dampers. Korkmaz *et al.* (2013) carried out probabilistic seismic risk assessment of hall structures composed of steel space frames in the upper side and RC moment frames in the lower side.

The literature survey showed that the seismic risk assessment has been effectively used to evaluate seismic performance of special or newly developed structure systems. It is also applied to identify optimum retrofit method for existing structures. In this study the seismic risk assessments of six- and twelve-story RC staggered wall system structures with middle corridors were performed. The seismic performances of staggered wall structures with added columns along the central corridor and the structures with their first story walls replaced with beams and columns were also compared with those of the regular staggered wall structures. Incremental dynamic analyses were carried out using twenty two pairs of earthquake records to obtain the failure probabilities and seismic risk for various intensities of seismic load. The spectral accelerations of earthquakes with various return periods and their probability density functions were obtained from the seismic hazard map of Korean Peninsula. The seismic risks of model structures were obtained from the seismic fragility and the hazard function of the model structures. Based on the incremental dynamic analysis results obtained using twenty two pairs of earthquakes the seismic fragility and risk of the model structures were assessed, and the robustness of the original and the modified staggered wall structures with enhanced redundancy were compared to confirm the effectiveness of the added interior columns.

2. Seismic risk assessment procedure

Seismic risk assessment is to quantify the potential damages and losses due to earthquakes and their probabilities of occurrence in a given period. It consists of analyzing seismic hazard, which describes earthquake phenomena that have potential to cause damage, and assessing structural vulnerability, which is the sensitivity of the structure to the expected seismic hazard. Structural vulnerability is the probability of damage to a structure given the level of earthquakes, which is

generally represented by fragility curves. The results of risk assessment provide probabilities for damage of buildings, which depends on their configurations and structural conditions.

Fragility curves, which are generally modeled as lognormal cumulative density functions, show the probability of a system reaching a limit state as a function of some measure of seismic intensity. In this study pseudo spectral acceleration was used as the seismic intensity measure, and the state of dynamic instability was considered as the limit state for failure. The seismic fragility is described by the conditional probability that the structural capacity, C , fails to resist the structural demand, D , given the seismic intensity hazard, SI , and is modeled by a lognormal cumulative distribution function as follows (Celik and Ellingwood 2009)

$$P[C < D | SI = x] = 1 - \Phi \left[\frac{\ln(\hat{C} / \hat{D})}{\sqrt{\beta_{D|SI}^2 + \beta_C^2 + \beta_M^2}} \right] \quad (1)$$

where $\Phi[\bullet]$ =standard normal probability integral, \hat{C} =median structural capacity, associated with the limit state, \hat{D} =median structural demand, $\beta_{D|SI}$ =uncertainty in D , β_C =uncertainty in C , and β_M =modeling uncertainty. FEMA P695 (2009) provides β_{TOT} , the total system collapse uncertainty, for the uncertainty in the normal probability integral function Φ in Eq. (1) based on the record-to-record uncertainty, design requirements related uncertainty, test data-related uncertainty, and the modeling uncertainty.

Seismic hazard quantifies the ground motions generated due to an earthquake. The likelihood of various levels of future intense ground motions at the site are represented in the standard way by the hazard function $H(S_a)$ as follows (Cornell *et al.* 2002)

$$H(S_a) = P[S_a \geq S_a] = k_0 S_a^{-k} \quad (2)$$

where S_a is the spectral acceleration, k_0 and k are coefficients determined by site characteristics. The equation implies that the hazard curve is linear on a log-log plot in the region of interest. In the previous research it was shown that typical values of the log-log slope k are 1 to 4 (Yun and Foutch 2000). In this study the coefficients are obtained using the design spectra of earthquakes with various return periods in Seoul area and their probabilities of occurrence. The probability of damage, i.e. the seismic risk of the structure, is obtained from the seismic fragility analysis and the hazard function as follows (Cornell *et al.* 2002)

$$P_{PL} = H(S_a^{\hat{C}}) \exp \left[\frac{k^2}{2} \sigma_{\ln S_a}^2 \right] \quad (3)$$

where $S_a^{\hat{C}}$ and $\sigma_{\ln S_a}^2$ are the median and variance of the spectral acceleration corresponding to the drift capacity for each damage state, respectively. They are obtained from the data set of spectral accelerations computed by nonlinear incremental time history analysis of model structures using the twenty two pairs of earthquake records. $S_a^{\hat{C}}$ is the median value of the spectral accelerations corresponding to the displacement of a specific damage state. $\sigma_{\ln S_a}^2$ is the variance of the acceleration responses corresponding to the specific damage state when they are fitted into the log-normal distribution. They are determined in the process of fragility analysis.

3. Seismic performance evaluation of model structures

3.1 Design and analysis modeling of example structures

The analysis model structures are six- and twelve-story staggered wall structures along the transverse (short) direction and are moment resisting structures along the longitudinal (long) direction. Along the transverse direction the structure was varied into three different types depending on the existence of interior columns.



Fig. 1 3D-view of 6-story analysis models

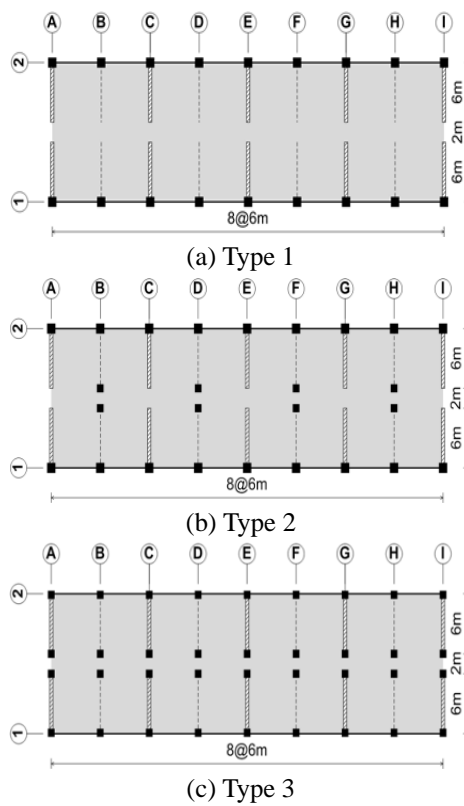


Fig. 2 First story structural plans of 6-story analysis models

Fig. 1 shows the configuration of the 6-story Type 1 and Type 3 model structures. Fig. 2 and Fig. 3 illustrate the first story structural plans and the elevation views of the three-types of model structures, respectively. Type 1 structure represent the basic form of a staggered wall structure with columns along the perimeter of the longitudinal direction and staggered walls located between two perimeter columns along the short directions. In the Type 2 structure the staggered walls in the first story were replaced by beams and interior columns along the corridor to accommodate wider open space in the ground floor. In the Type 3 structure interior columns were added to the Type 1 structure throughout the stories. In all model structures, 200×600 mm beams were located between two staggered walls along the transverse direction above the middle corridor. The thickness of the staggered walls is 200 mm throughout the stories in every model structure. The structures were designed with dead and live loads of 7.0 kN/m² and 2.5 kN/m², respectively, and the design seismic load was determined using the response acceleration coefficients S_{DS} and S_{D1} of 0.37 and 0.15, respectively, based on the ASCE/SEI 7-10 (2010). The model structures were assumed to be residential buildings with floor panel heating system and thicker slab to minimize vertical noise and vibration transmission, which result in relatively large dead load compared with ordinary

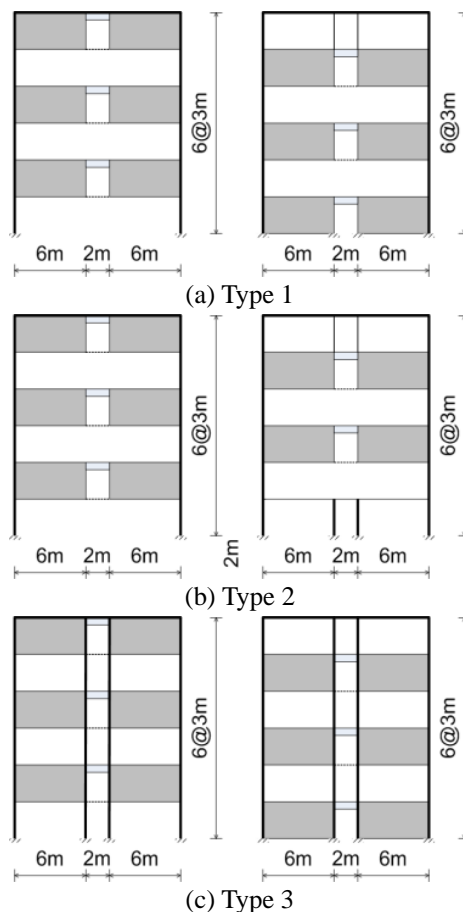


Fig. 3 Elevation of 6-story analysis models

office buildings. The response modification factor for seismic load was assumed to be 3.0 considering the fact that the system is not defined as one of the seismic load-resisting systems in design codes. The ultimate strengths of concrete and reinforcing steel are 27 MPa and 400 MPa, respectively. The design base shears of the model structures are shown in Table 1. Table 2 shows the fundamental natural periods of the model structures along the transverse direction calculated by eigen-value analysis. It can be observed that the natural periods of the Type 2 structures, in which the first story staggered walls were replaced by beams and columns, increased by 38% in the 6-story structure and by 8% in the 12-story structure compared with those of the Type 1 structures. The natural periods of the Type 3 structures with added interior columns throughout the stories decreased by 27% in the 6-story structure and by 19% in the 12-story structure compared with those of the Type 1 structures.

Table 1 Design base shear of analysis models

| Model structures | Seismic response coefficient | Total effective weight (kN) | Design base shear (kN) |
|------------------|------------------------------|-----------------------------|------------------------|
| Type 1 | 6F | 36760.17 | 5036.120 |
| | 12F | 75565.37 | 6165.578 |
| Type 2 | 6F | 36737.58 | 5033.048 |
| | 12F | 75604.24 | 6161.745 |
| Type 3 | 6F | 36608.85 | 5015.412 |
| | 12F | 75424.43 | 6147.09 |

Table 2 Natural periods of analysis model structures along the transverse direction

| Model structures | Natural period | |
|------------------|----------------|-------|
| Type 1 | 6F | 0.293 |
| | 12F | 0.666 |
| Type 2 | 6F | 0.404 |
| | 12F | 0.717 |
| Type 3 | 6F | 0.214 |
| | 12F | 0.542 |

The analytical model for the connecting beams located above the corridor and between two walls is composed of two elastic beam elements, two moment hinges, and a shear hinge in the middle as shown in Fig. 4. The properties of the moment and shear hinges are defined based on the ASCE/SEI 41-06 (2007) and Englekirk (2003), respectively. The probable flexural strength, M_{pr} , is obtained from the nominal moment strength multiplied by the overstrength factor, and the shear strength is computed as follows

$$V_u = \frac{2M_{pr}}{L} \quad (4)$$

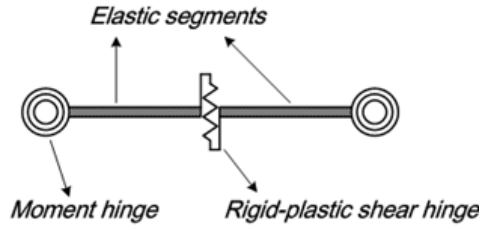


Fig. 4 Analysis model for a link beam

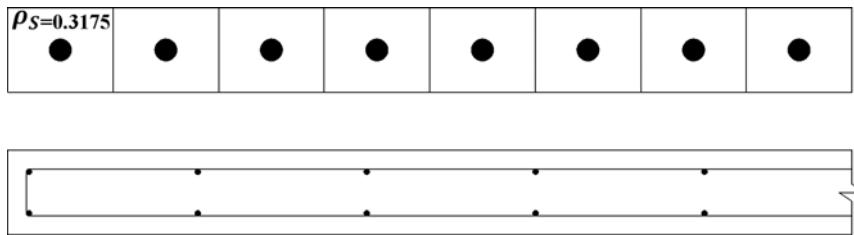


Fig. 5 Auto-size fiber section for shear wall elements

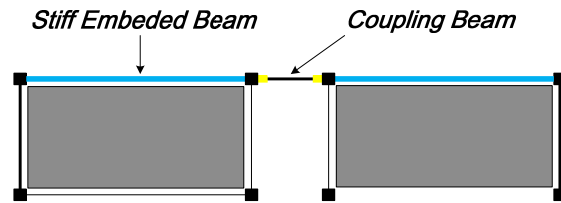


Fig. 6 Installation of embedded beams at the top of staggered walls

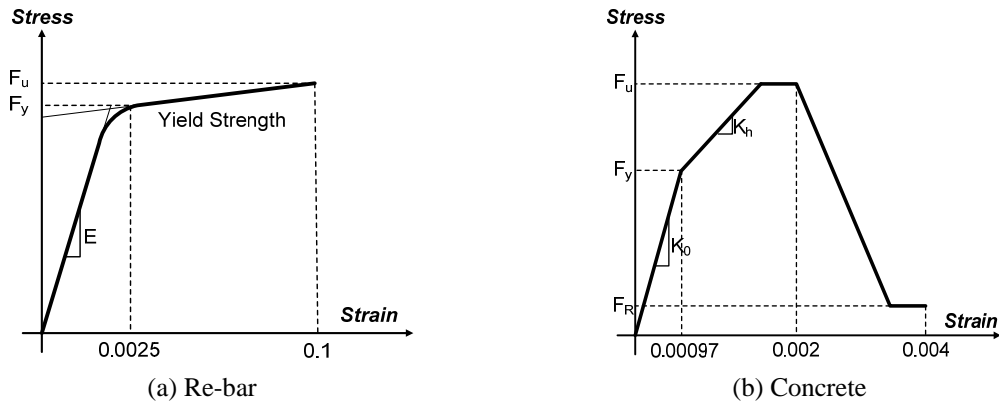


Fig. 7 Stress-strain relationships of staggered wall element

where L is the length of the member. The staggered walls were modeled by the Shear Wall fiber elements provided in the Perform 3D (2006). Each Shear Wall element was modeled using eight fibers with 0.3175% reinforcement in each fiber as shown in Fig. 5. In the model the yield and the ultimate strength of concrete are 27 MPa and 18MPa, respectively, and the residual strength is defined as 20% of the ultimate strength. The strain at the ultimate strength is 0.002, and the

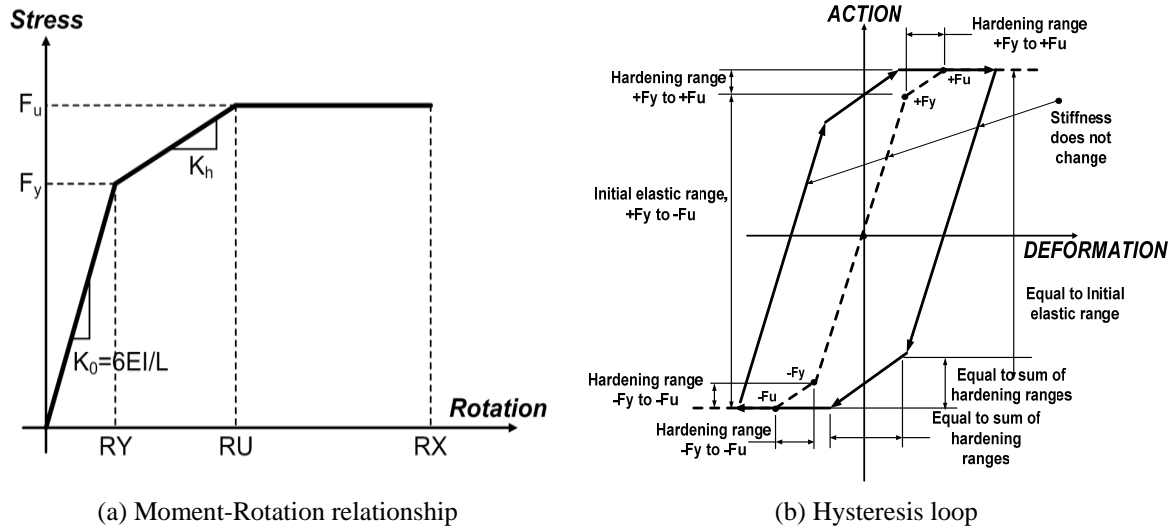


Fig. 8 Non-linear force-deformation model for columns

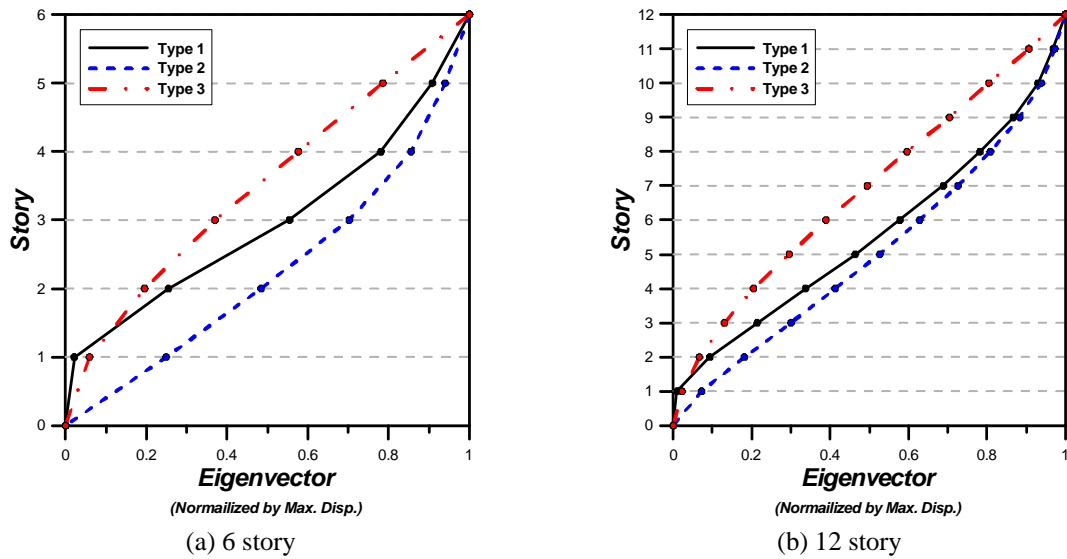


Fig. 9 Fundamental mode shapes of model structures used in the pushover analyses

ultimate strain is defined as 0.004. The reinforcing steel is modeled with bi-linear lines, and the overstrength factors of 1.5 and 1.25 are used for concrete and reinforcing steel, respectively. As the shear wall element has no in-plane rotational stiffness at its nodes, a beam element was embedded in the wall as shown in Fig. 6 to specify a moment-resisting connection between a beam and a wall. Fig. 7(a) and 7(b) shows the stress-strain relationship of re-bars and reinforced concrete proposed by Paulay and Priestly (1992), respectively. The behavior of re-bars was represented by bi-linear curve, and the yield stress and the residual stress of concrete were assumed to be 60% and 20% of the ultimate strength, respectively. Fig. 8 shows the nonlinear models for columns subjected to monotonic and cyclic loads based on the recommendation of ASCE/SEI 41-06.

3.2 Nonlinear static analysis of model structures

To evaluate overall strength and failure mode of model structures, nonlinear static pushover analyses of the model structures were carried out using the lateral load pattern proportional to the fundamental model shape of the model structures (Fig. 9). The nonlinear analysis is conducted using the program code Perform 3D (2006), and Fig. 10 shows the pushover curves of the model structures. It can be observed that the Type 1 and Type 2 structures showed similar overall behaviors, which implies that the replacement of the first story staggered walls with beams and columns does not affect the stiffness and strength of the structure significantly. This implies that, by removing staggered walls in the first story, large open space can be created without sacrificing structural integrity. However the Type 3 structure with added interior columns along the corridor showed significantly higher stiffness and strength. Fig. 11 depicts the locations of plastic hinges in the 12-story model structures when their strengths reached the maximum values. It can be observed that in the Type 1 and Type 2 structures plastic hinges formed mainly at the lower story exterior columns and connection beams. It was noticed that the sudden strength drop in each model structure was initiated by the large plastic rotations at the exterior columns. On the other hand the plastic hinge distribution of the Type 3 structure is quite different. It can be observed that the plastic hinges are relatively evenly distributed throughout the stories and that severe plastic deformation occurred mainly in the connection beams rather than in the columns. A few plastic hinges can be observed in the lower story exterior columns; however the plastic rotations are only minute. Compared with the failure mode of Type 1 and Type 2 structures, in which plastic hinges were mostly concentrated in the lower few stories, the wider distribution of plastic hinges in the Type 3 structure contributes to significant increase in strength.

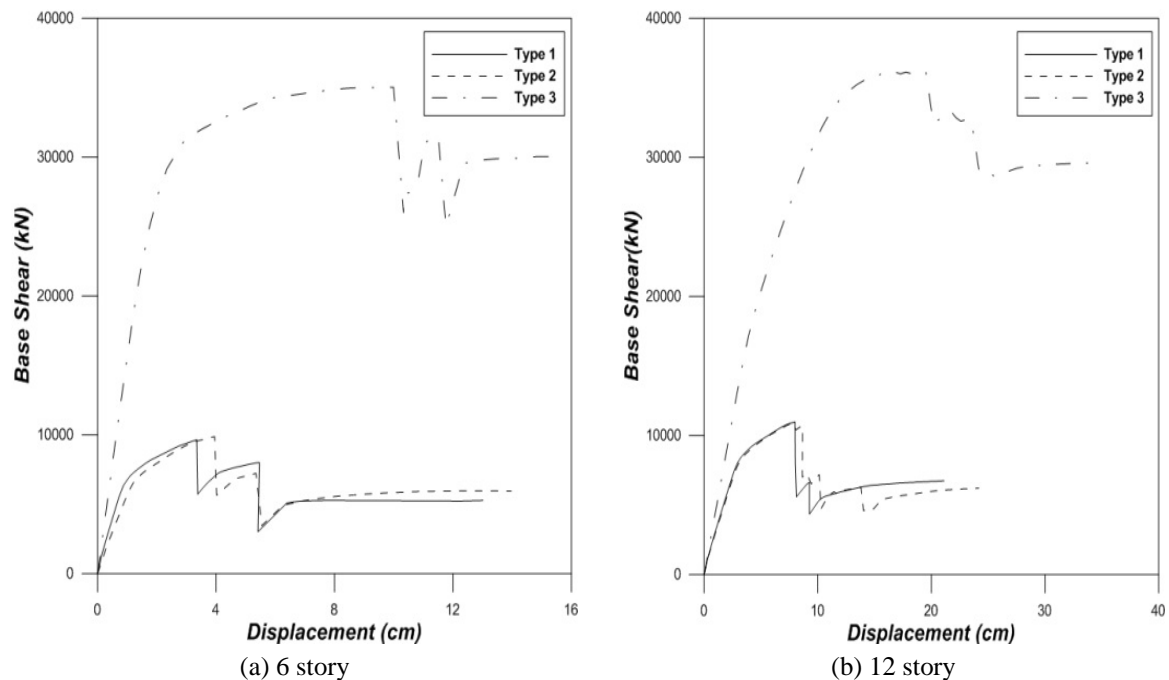


Fig. 10 Pushover curves of the model structures

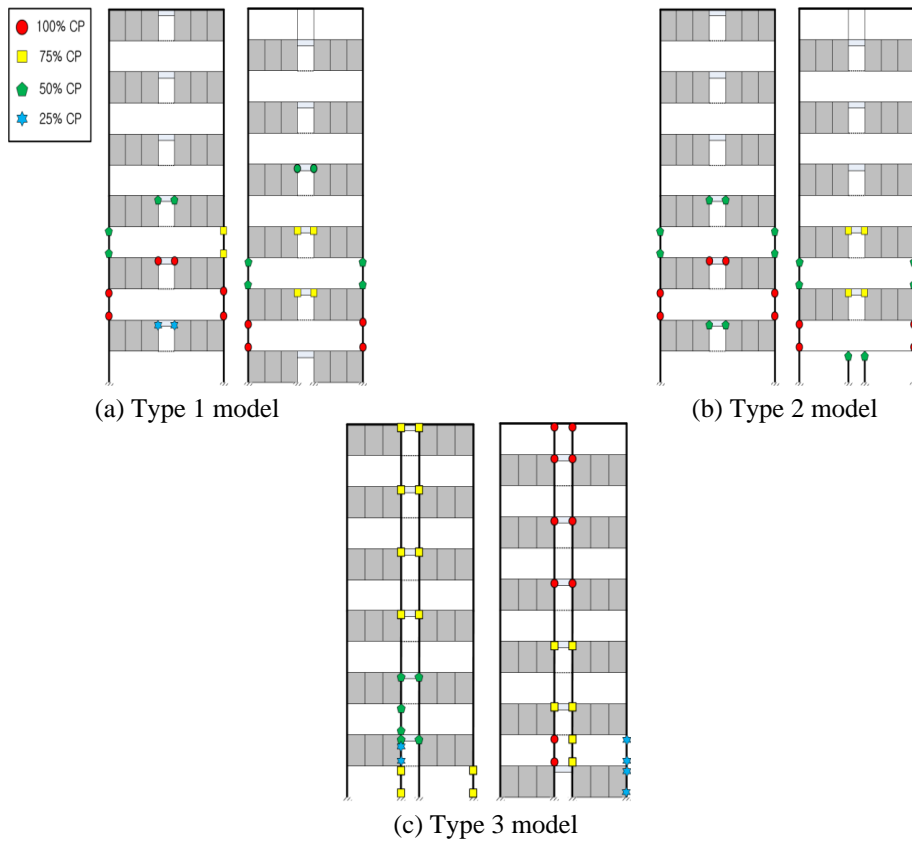


Fig. 11 Plastic hinge distribution of the 12-story structure at the maximum strength

3.3 Seismic fragility analysis of model structures

Nonlinear incremental dynamic analyses were conducted using the 22 pairs of the far field ground motions provided by the FEMA P695 (2009) to establish the median and the standard deviation of the collapse capacity of each analysis model. The ground motions are scaled to a specific ground motion intensity such that the median spectral acceleration of the record set matches the spectral acceleration at the fundamental period of the model structure. This scaling process corresponds to the ground motion scaling requirements of ASCE/SEI 7-10 (2010). Fig. 12 shows the response spectra of the scaled earthquake records used in the analysis and Fig. 13 depicts the incremental dynamic analysis results of the model structures. In this study the total system collapse uncertainty, β_{TOT} , provided in the FEMA P695, was used for the uncertainty in the lognormal cumulative distribution function shown in Eq. (1). The design requirement related uncertainty and the test data-related uncertainty were assumed to be ‘Good’ and ‘Fair’, respectively, and the modeling uncertainty was assumed to be ‘Good’. This results in the total system collapse uncertainty of 0.6, which was used throughout this study.

The probability of reaching the limit states and the corresponding fragility curves were drawn for four different damage states defined in the HAZUS (1997), which are Slight, Moderate, Extensive, and Complete damages. The Slight damage is the state with minute cracks, and the

Moderate damage is the state with formation of wide spread cracks with partial yielding. In the Extensive damage state part of the structure has reached ultimate states, and in the Complete

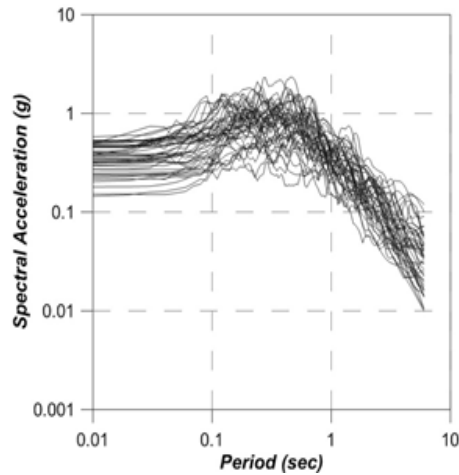


Fig. 12 Response spectra of the 44 earthquake records used in the dynamic analysis

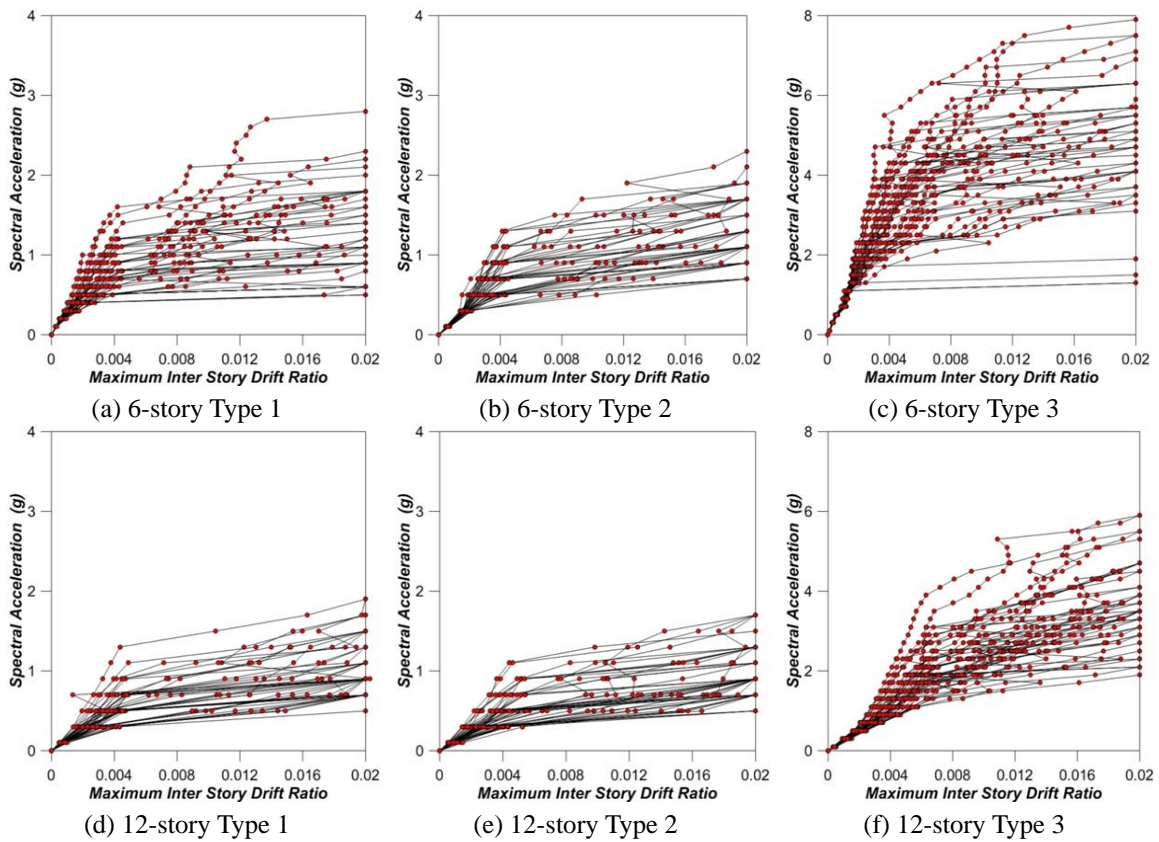


Fig. 13 IDA curves of the 6- and 12-story model structures

Table 3 Seismic fragility factors of analysis models at four different damage states

| | | Slight | | Moderate | | Extensive | | Complete | |
|--------|-----|-----------------|--------------------|-----------------|--------------------|-----------------|--------------------|-----------------|--------------------|
| | | $S_a^{\bar{C}}$ | $\sigma_{lnS_a}^2$ | $S_a^{\bar{C}}$ | $\sigma_{lnS_a}^2$ | $S_a^{\bar{C}}$ | $\sigma_{lnS_a}^2$ | $S_a^{\bar{C}}$ | $\sigma_{lnS_a}^2$ |
| Type 1 | 6F | 0.24g | 0.126 | 0.53g | 0.223 | 0.72g | 0.242 | 0.98g | 0.348 |
| | 12F | 0.12g | 0.180 | 0.33g | 0.251 | 0.58g | 0.278 | 0.78g | 0.368 |
| Type 2 | 6F | 0.21g | 0.113 | 0.30g | 0.148 | 0.41g | 0.224 | 0.74g | 0.417 |
| | 12F | 0.14g | 0.228 | 0.27g | 0.287 | 0.38g | 0.322 | 0.54g | 0.365 |
| Type 3 | 6F | 0.69g | 0.120 | 1.82g | 0.185 | 2.43g | 0.234 | 4.03g | 0.247 |
| | 12F | 0.46g | 0.121 | 0.87g | 0.208 | 1.11g | 0.247 | 1.92g | 0.287 |

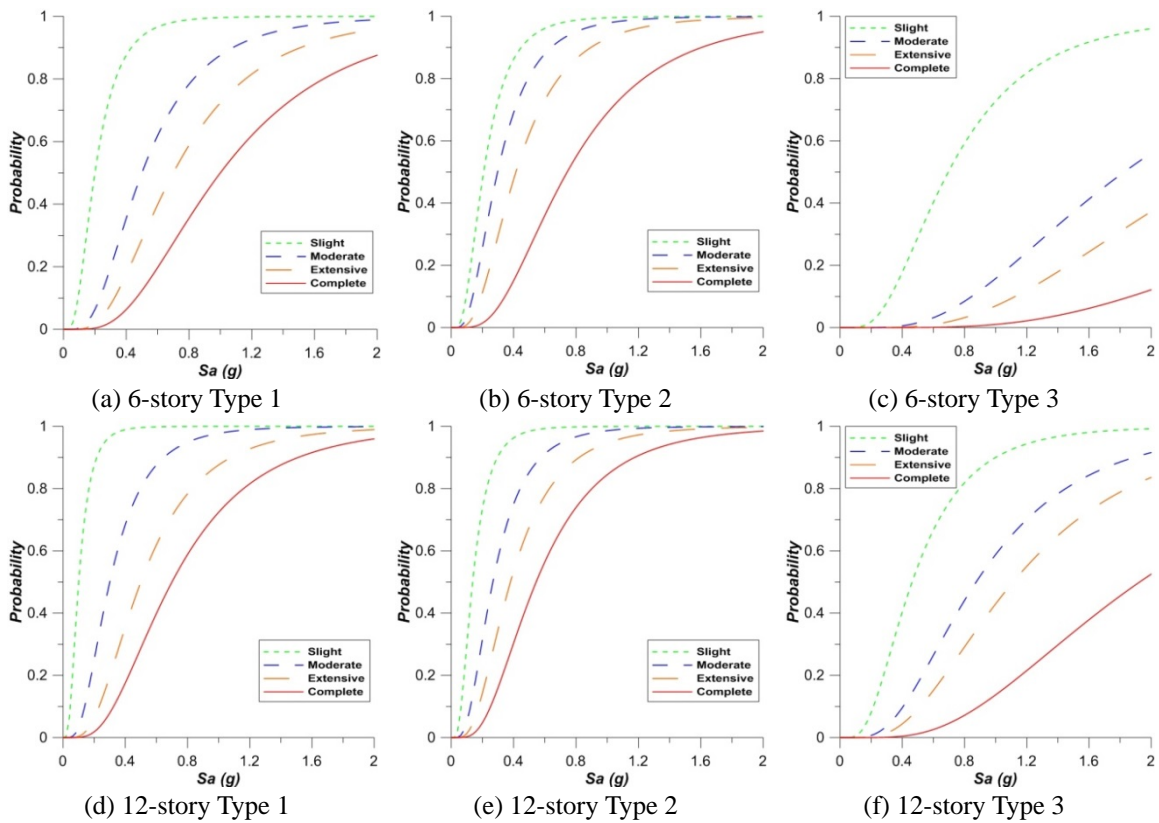


Fig. 14 Fragility curves of analysis models

damage state the structure is near collapse. In this study the criteria for the Slight and the Moderate damage states were defined as the inter-story drifts corresponding to 70% and 100% of the yield point, respectively, when the load-displacement relationship was idealized as bi-linear curves. The Complete damage was defined as the state where the maximum strength was reached, and the Extensive damage state was defined as the inter-story drift at a quarter point between the Moderate and the Complete damage state. Fig. 14 depicts the fragility curves of the 6- and 12-story analysis

model structures obtained from the IDA results. It can be observed that the probabilities of reaching the limit states are slightly higher in the 12-story structures than those in the 6-story structures. The fragilities are largest in the Type 2 structures which have no walls in the first story and are smallest in the Type 3 structures in which additional interior columns are installed along the middle corridor. It was observed in the pushover analysis results that in the Type 3 structures the plastic hinges formed in the connecting beams between two staggered walls were more widely distributed along the height of the structures due to installation of the interior columns. Table 3 shows the required parameters of the fragility analysis, where it can be observed that the spectral accelerations at each damage state of the 6-story structures are higher than those of the 12-story structures.

3.4 Seismic risk analysis of staggered wall structures

Seismic risk analysis of a structure requires the information of seismic hazard which is the likelihood of experiencing earthquake shaking of a certain intensity in a specific region. In this study the probability of an earthquake with a certain intensity in Seoul area was estimated using the seismic hazard map developed based on the historical and instrumental earthquake data. Fig. 15 depicts the seismic hazard map of Korean peninsula for an earthquake with return period of 1,000 years (EESK, 1997), and Fig. 16 shows the response spectra for earthquakes with 10% probability of occurrence in 5, 10, 20, 50, 100, 250, and 480 years in Seoul area. If PE_N is defined as the probability of occurrence in N years, the probability of occurrence in one year period, PE_1 , can be obtained as follows

$$PE_1 = 1 - (1 - PE_N)^{1/N} \quad (5)$$

Table 4 shows the annual probability of exceedance of an earthquake in Seoul area with various return periods obtained from Eq. (5). The seismic hazard curve was evaluated using the probability

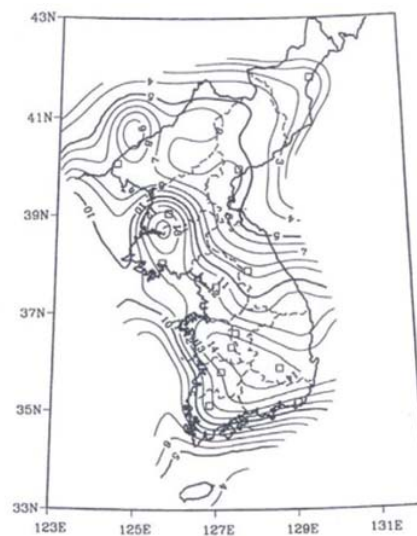


Fig. 15 Seismic hazard map of Korea (for earthquakes with return period of 1000 years)

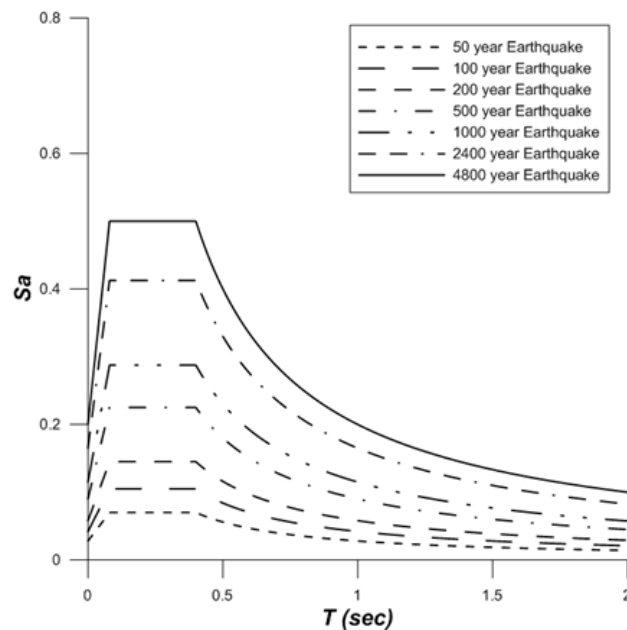


Fig. 16 Response spectra of earthquakes with various return periods in Seoul area

Table 4 Annual probability of exceedance of earthquakes with various return periods

| Exceedance probability/Period | Annual probability (PE_1) |
|-------------------------------|-------------------------------|
| 10% / 5years | 0.02085 |
| 10% / 10years | 0.01048 |
| 10% / 20years | 0.00525 |
| 10% / 50years | 0.00210 |
| 10% / 100years | 0.00105 |
| 10% / 250years | 0.00042 |
| 10% / 480years | 0.00022 |

of occurrence obtained from Eq. (5) and the response spectra constructed based on the hazard map. Fig. 17 shows the hazard curve of model structures obtained from regression analysis, which plots the response spectra and their annual probability of occurrence in log-log scale. It can be observed that the 6-story Type 1, 2, and 3 structures had almost the same hazard levels. This implies that the likelihoods of a certain level of ground motion at the site are almost the same. This is due to the fact that the spectral accelerations corresponding to the natural periods of the three structures fall on the same maximum value on the design spectrum. In the twelve-story structures, the likelihoods of a certain level of ground motion is largest in the Type 3 structure which has the shortest fundamental natural period due to the addition of the interior columns to the conventional staggered wall structure, and is the smallest in the Type 2 structure in which the staggered walls in the first story were replaced with beams and interior columns, and therefore has the longest natural period. Table 5 shows the coefficients k and k_0 obtained from the hazard curves, which are used to obtain the seismic risk.

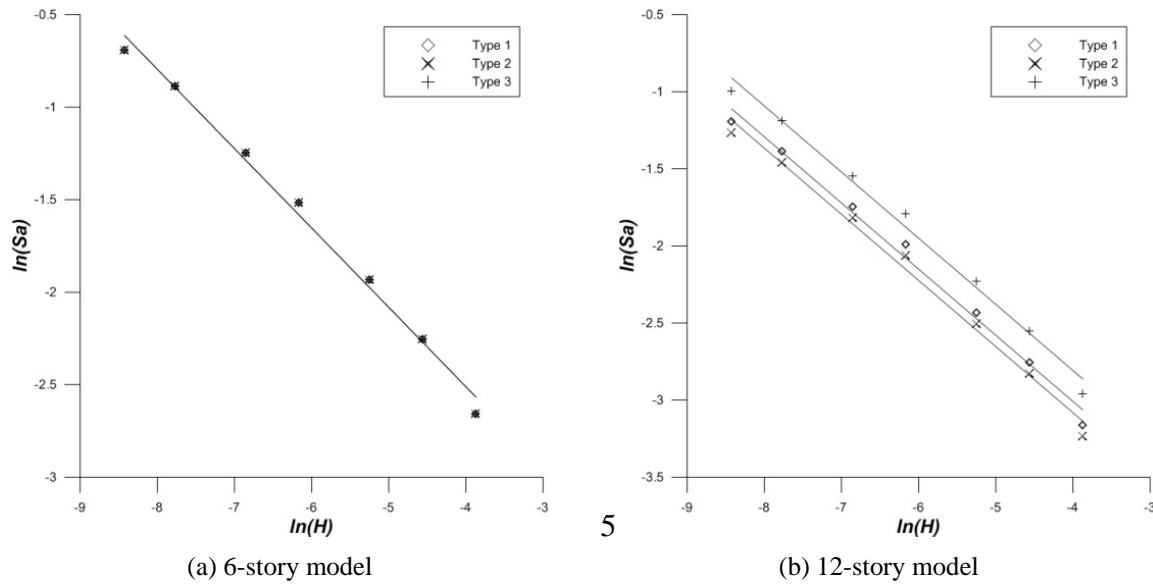


Fig. 17 Seismic hazard curve for analysis models

Table 5 Coefficients for the hazard function obtained from regression analysis

| Model structures | | k | k_0 |
|------------------|-----|--------|----------|
| Type 1 | 6F | 2.3315 | 0.000053 |
| | 12F | 2.3315 | 0.000016 |
| Type 2 | 6F | 2.3315 | 0.000053 |
| | 12F | 2.3315 | 0.000014 |
| Type 3 | 6F | 2.3315 | 0.000053 |
| | 12F | 2.3315 | 0.000026 |

Figs. 18 and 19 show the probability of each damage state being exceeded, which is called the seismic risk, in one and in 50-years, respectively, obtained by using Eq. (3). The coefficient k in Eq. (3) was computed by regression analysis of the seismic hazard data, and the required variables were obtained from the fragility analysis results shown in Fig. 11. It can be observed that in the 6-story structures the seismic risks for all damage states are highest in the Type 2 structure, and are lowest in the Type 3 structure. The difference in seismic risk is very large in the slight damage state, but gradually decreases as the damage state becomes severe. In the 12-story structures, the seismic risk of the Type 1 structure is larger than that of the Type 2 structure in the slight damage state. From the moderate damage state to collapse the seismic risks of the Type 2 structure become largest as in the 6-story structure. The risks of the 12-story structures are generally slightly larger than those of the 6-story structures in the slight damage state. However the seismic risks of the 12-story structures in the more severe damage states are slightly smaller than those of the 6-story structures. The trends are similar in the earthquakes with annual and 50-year probabilities of exceedance. However the risk of damage for the 50 year earthquake is significantly larger than the annual risk of damage in every damage state.

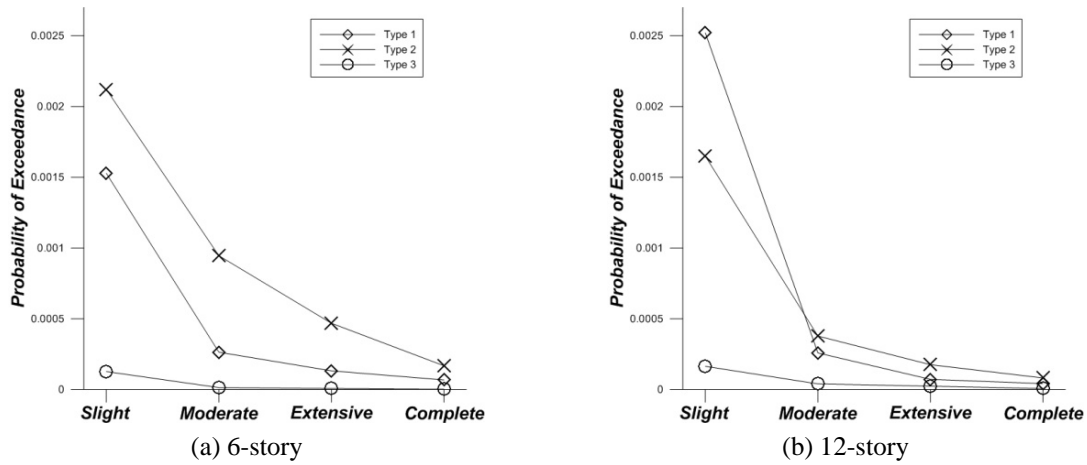


Fig. 18 Annual probability of exceedance

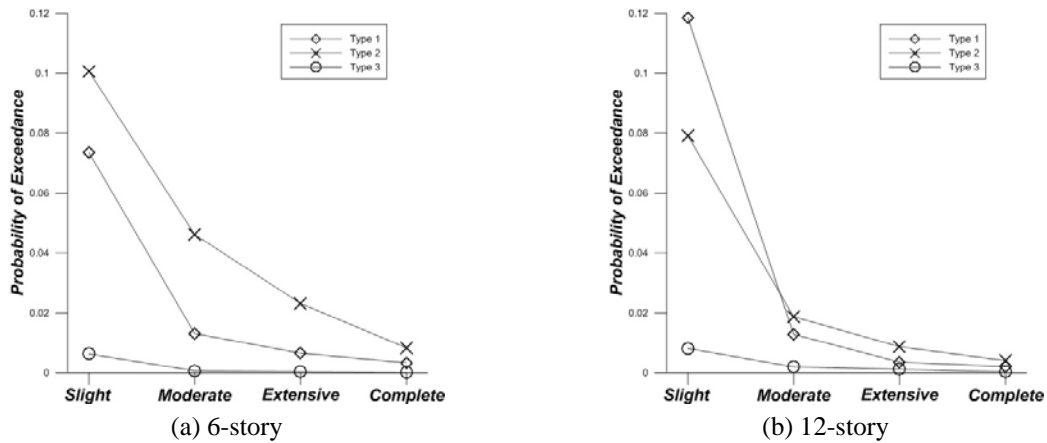


Fig. 19 Probability of exceedance in 50 years

4. Conclusions

This study carried out the seismic risk assessment of six- and twelve-story reinforced concrete staggered wall system structures designed with three different structural variations. The performances of model structures with added columns along the central corridor and the structures with their first story walls replaced by beams and columns were compared with those of the regular staggered wall structures. Fragility curves were drawn from the results of incremental dynamic analyses using twenty two pairs of earthquake records. The seismic risk for each damage state was computed based on the fragility analysis results and the probability of occurrence of earthquake ground motions in Seoul area.

According to the analysis results, the addition of interior columns (Type 3 structures) to the regular staggered wall structures (Type 1 structures) resulted in significant increase in the overall robustness of the model structures. The structures with their first story staggered walls replaced by beams and columns, Type 2 structures, showed similar strength and ductility to the prototype

structure. However the Type 2 structures showed higher fragility and risk than the regular structures, especially in the twelve-story structure. The seismic fragility and risk of the Type 3 structures with enhanced redundancy turned out to be significantly smaller than those of the other structures. The difference in seismic risk among the three alternatives was largest in the slight damage state, and gradually decreased as the damage state became more severe. The difference was generally larger in the twelve-story structures than in the six-story structures. Based on the analysis results, it was concluded that the overall seismic risk of regular staggered wall structures would be significantly reduced and the seismic robustness significantly increased when the structural redundancy of the model structure is increased by adding interior columns along the middle corridor.

Acknowledgements

This work (No. 2011-0015734) was supported by Mid-career Researcher Program through National Research Foundation grant funded by the Korea Ministry of Education, Science and Technology.

References

- ASCE (2010), *Minimum design loads for buildings and other structures*, ASCE Standard ASCE/SEI 7-10, American Society of Civil Engineers, Reston, Virginia.
- ASCE (2007), *Seismic rehabilitation of existing buildings*, ASCE Standard ASCE/SEI 41-06, American Society of Civil Engineers, Reston Virginia.
- Celik, O.C. and Ellingwood, B.R. (2009), "Seismic risk assessment of gravity load designed reinforced concrete frames subjected to mid-america ground motions", *J. Struct. Eng.*, **135**(4), 414-424.
- Computer and Structures(2006), *PERFORM components and elements for PERFORM 3D and PERFORM-Collapse ver.4*, CSI, Berkeley, CA.
- Cornell, C.A., Jalayer, F., Hamburger, R. and Foutch, D. (2002), "Probabilistic basis for 2000 SAC federal emergency management agency steel moment frame guidelines", *J. Struct. Eng.*, **128**(4), 526-533.
- EESK (1997), *Research on seismic design code (II)*, Korea Ministry of Construction and Transportation.
- Ellingwood, B.R. (2001), "Earthquake risk assessment of building structures", *Reliab. Eng. Syst. Safe.*, **74**, 251-262.
- Ellingwood, B.R. and Wen, Y.K. (2005), "Risk-benefit-based design for low-probability/high consequence earthquake events in Mid-America", *Prog. Struct. Eng. Mater.*, **7**, 56-70.
- Englekirk, R. (2003), *Seismic design of reinforced and precast concrete buildings*, John Wiley & Sons, Inc.
- Erberik, M.A. and Elnashai, A.S. (2004), "Fragility analysis of flat-slab structures", *Eng. Struct.*, **26**, 937-948.
- FEMA P695 (2009), *Quantification of building seismic performance factors*, Federal Emergency Management Agency, Washington, D. C.
- HAZUS (1997), *Earthquake loss estimation methodology*, Technical Manual, National Institute of Building for the Federal Emergency Management Agency, Washington D.C.
- Kennedy, R.P. and Ravindra, M.K. (1984), "Seismic fragilities for nuclear power plant risk studies", *Nuclear Eng. Des.*, **79**, 47-68.
- Korkmaz, K.A, Ay, Z., Sari, A. and Celik, I.D. (2013), "Probabilistic seismic risk assessment of hall buildings in Turkey", *Struct. Des. Tall Spec.*, **22**(5), 415-439.
- Lee, J. and Kim, J. (2013), "Seismic performance evaluation of staggered wall structures using Fema P695

- procedure”, *Mag. Concrete Res.*, **65**(17), 1023-1033.
- Paulay, T. and Priestely, M.J.N. (1992), Seismic design of reinforced and masonry building.
- PEER (2006), *PEER NGA database*, Pacific Earthquake Engineering Research Center, University of California, Berkeley, U.S.A, <http://peer.berkeley.edu/nga/>.
- PERFORM-3D (2006), “Nonlinear analysis and performance assessment for 3D structures-user guide”, Berkeley(CA, USA), Computers and Structures.
- Ramirez, C.M., Lignos, D.G., Miranda, E. and Kolios, D. (2012), “Fragility functions for pre-Northridge welded steel moment-resisting beam-to-column connections”, *Eng. Struct.*, **45**, 574-584.
- Seismic performance criteria (1997), *Research on seismic design code (II)*, Korea Department of Construction and Transportation.
- Shinozuka, M., Feng, M.Q., Lee, J. and Naganuma, T. (2000), “Statistical analysis of fragility curves”, *J. Eng. Mech.*, **126**(12), 1224-1231.
- Sørensen, J.D. (2011), “Framework for robustness assessment of timber structures”, *Eng. Struct.*, **33**, 3087-3092.
- Tafakori, E., Banazadeh, M., Jalali, S.A. and Tehranizadeh, M. (2013), “Risk-based optimal retrofit of a tall steel building by using friction dampers”, *Struct. Des. Tall Spec.*, **22**, 700-717.
- Taflanidis, A.A. and Jia, G.F. (2011), “A simulation-based framework for risk assessment and probabilistic sensitivity analysis of base-isolated structures”, *Earthq. Eng. Struct. Dyn.*, **40**, 1629-1651.
- Yun, S.Y. and Foutch, D.A. (2000), “Performance prediction and evaluation of low ductility steel moment frames for seismic loads”, SAC Background Rep. No. SAC/BD-00/26, SAC Joint Venture, Richmond, Calif.

IT